

Enhancement in Light Extraction Efficiency of GaN-Based Light-Emitting Diodes Using Double Dielectric Surface Passivation

Chung-Mo Yang¹, Dong-Seok Kim¹, Yun Soo Park¹, Jae-Hoon Lee², Yong Soo Lee¹, Jung-Hee Lee¹

¹School of Electrical Engineering and Computer Science, Kyungpook National University, Daegu, South Korea

²GaN Power Research Group, R & D Institute, Samsung LED Co., Ltd., Suwon, South Korea

Email: jlee@ee.knu.ac.kr

Received June 27, 2012; revised July 26, 2012; accepted August 8, 2012

ABSTRACT

SiO₂/Al₂O₃ double dielectric stack layer was deposited on the surface of the GaN-based Light-Emitting Diode (LED). The double dielectric stack layer enhances both the electrical characteristics and the optical output power of the LED because the first Al₂O₃ layer plays a role of effectively passivating the p-GaN surface and the second lower index SiO₂ layer increases the critical angle of the light emitted from the LED surface. In addition, the effect of the Fresnel reflection is also responsible for the enhancement in output power of the double dielectric passivated LED. The leakage current of the LED passivated with Al₂O₃ layer was -3.46×10^{-11} A at -5 V, at least two and three orders lower in magnitude compared to that passivated with SiO₂ layer (-7.14×10^{-9} A) and that of non-passivated LED (-1.9×10^{-8} A), respectively, which indicates that the Al₂O₃ layer is very effective in passivating the exposed GaN surface after dry etch and hence reduces nonradiative recombination as well as reabsorption of the emitted light near the etched surface.

Keywords: GaN; Light-Emitting Diode (LED); Al₂O₃; PEALD; Passivation; Double Dielectric Stack Layer

1. Introduction

The III-nitrides are suitable materials for photoelectronic applications covering most of the electromagnetic spectrum due to their wide range of direct bandgap energy. Light emitting diodes (LEDs) are promising semiconductor devices for solid state lighting. Due to a remarkable development in LED fabrication technologies, the LEDs are now being commercialized in various applications such as traffic signals, full-color displays, back lighting in liquid-crystal displays, and so on [1]. However, further improvement in output power with long life time is still required for the GaN-based LED to be more efficiently used in such a field. The increase of the external quantum efficiency (η_{EQE}), which can be determined from the product of injection efficiency (η_{inj}) \times radiative efficiency (η_{rad}) \times extraction efficiency (η_{ext}), is the most important factor in achieving a high efficiency LED. η_{inj} and η_{rad} can be increased by improving the crystal quality and optimizing the epitaxial layer structure which maximizes the radiative recombination in active region. Surface passivation with appropriate dielectric layers is also necessary to avoid non-radiative recombination for high η_{rad} [2]. Special techniques such as control of surface roughness [3-5], preparation of patterned sapphire substrate

(PSS) [6,7], application of flip-chip bonding [8-10], adaption of laser lift-off process [11], and formation of photonic crystal structure [12] are frequently used to improve η_{ext} , which can be increased by increasing the critical angle for the emitted light through an appropriate modification of the surface of the LED [13,14]. Anti-reflection (AR) coating of dielectric layers is frequently used to reduce the Fresnel reflection at the semiconductor-air interface in communication LEDs.

In this work, we report, in more detail, the development of passivation technique for the GaN-based LEDs by using double dielectric stack layer design is not optimized for the maximum anti-reflectivity.

2. Device Fabrication

Figure 1(a) shows the schematic LED configuration investigated in this work. The layer structure was grown on the patterned sapphire substrate (PSS) by metal-organic chemical vapor deposition (MOCVD). The blue LED structure contains low temperature grown GaN buffer layer, un-doped GaN layer, Si doped n-GaN layer, InGaN/GaN multi-quantum well active layer and Mg doped p-GaN cladding layer. The composition and thickness of InGaN/GaN multi-quantum well active layer was opti-

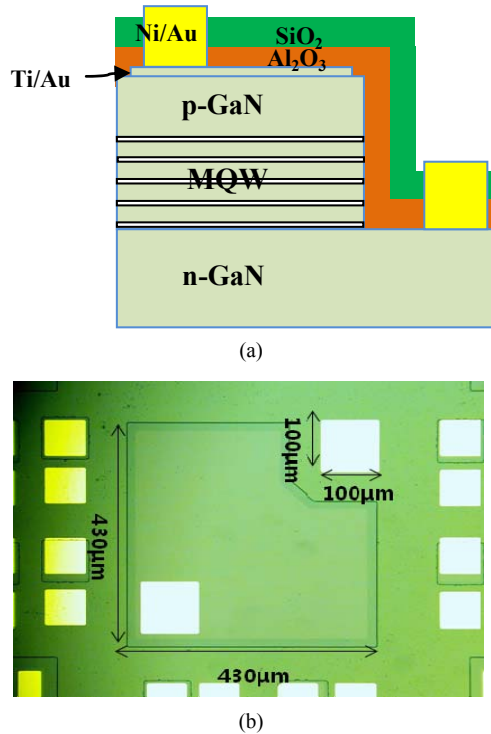


Figure 1. The schematic of the LED configuration investigated in this work (a); and the fabrication of the $430\ \mu\text{m} \times 430\ \mu\text{m}$ size real LED chip (b).

mized for emission wavelength of $\sim 460\ \text{nm}$. **Figure 1(b)** shows the fabricated LED chip with size of $430\ \mu\text{m} \times 430\ \mu\text{m}$.

The window for n-electrode was first defined by dry etching and a transparent electrode consisting of Ni/Au ($50\ \text{\AA}/50\ \text{\AA}$) was deposited on p-GaN layer, which was followed by rapid thermal annealing at 500°C (at N_2/O_2 ambient) for ohmic contact between the transparent electrode and p-GaN top layer. Thick Ti/Au bonding pads with thickness of $300\ \text{\AA}/4000\ \text{\AA}$ was then deposited. The double dielectric stack layer, which consists of $5\ \text{nm}$ -thick Al_2O_3 layer [15] deposited by plasma-enhanced atomic layer deposition (PEALD) and $50\ \text{nm}$ -thick SiO_2 layer deposited by plasma-enhanced chemical vapor deposition (PECVD), was sequentially deposited on the surface of the LED to complete the fabrication process. The PEALD method has the advantages such as an excellent uniformity, a high quality film density, a controllability of atom level thickness and the perfect surface step coverage for the LED structure due to the self-limiting deposition characteristic. A gas phase reaction can be suppressed among the injected reactant. Therefore, a thin film layer is formed by a saturated surface reaction therefore the low temperature deposition is possible. In addition, to evaluate the interface trap density between SiO_2 or Al_2O_3 layer and p-GaN layer, the MOS capacitors with anode pattern of $300\ \mu\text{m}$ diameter and virtual ground contact [16] were also fabri-

cated. For comparison, three different LEDs were also prepared; $5\ \text{nm}$ -thick single Al_2O_3 -passivated, $50\ \text{nm}$ -thick single SiO_2 -passivated, and non-passivated LED.

3. Optimization of Double Dielectric Stack Layer

To maximize the optical output power, the refractive index and the thickness of a dielectric layer, were estimated from the concept based on the Fresnel reflection for the antireflection. The Fresnel reflection at the interface can be reduced to zero, assuming normal incidence, when an anti-reflective dielectric layer is inserted between air and semiconductor, which has the following relations:

$$\text{Refractive index} : n_{\text{AR}} = \sqrt{n_{\text{S}} \times n_{\text{A}}} \quad (1)$$

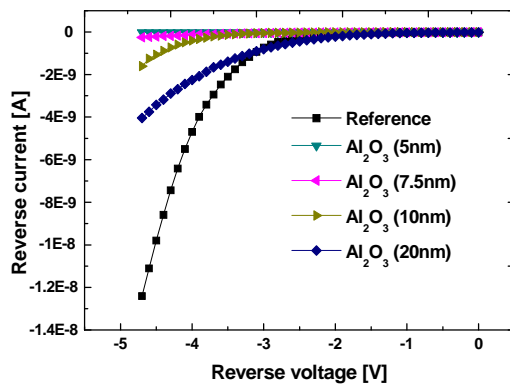
and

$$\text{thickness} = \frac{\lambda}{4} = \frac{\lambda_0}{4n_{\text{AR}}} \quad (2)$$

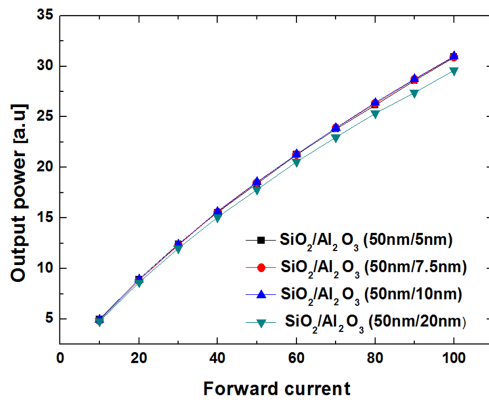
where n_{AR} is a refractive index of anti-reflection layer, n_{S} is a refractive index of semiconductor, n_{A} is a refractive index of air, and λ is wavelength, respectively. The estimated refractive index and the thickness of an anti-reflection layer is 1.55 and $\sim 70\ \text{nm}$, respectively, when the semiconductor is GaN and the emission wavelength λ is $460\ \text{nm}$. To obtain n_{AR} of 1.55 with double dielectric stack layer, such as Al_2O_3 (refractive index of 1.77)/ SiO_2 (refractive index of 1.46) investigated in this work, the thickness ratio between two dielectric layers is approximately $7(\text{SiO}_2):3(\text{Al}_2\text{O}_3)$, which approximately corresponds to the SiO_2 thickness of $50\ \text{nm}$ and the Al_2O_3 thickness of $20\ \text{nm}$. However, the $5\ \text{nm}$ -thick Al_2O_3 layer was used for the double layer in this work, instead of the calculated value of $20\ \text{nm}$ because the reverse current characteristics of the Al_2O_3 -passivated LED become rapidly degraded as the thickness increases as shown in **Figure 2(a)** (the leakage current of the 5 and $20\ \text{nm}$ thick Al_2O_3 passivated layer were $-3.46 \times 10^{-11}\ \text{A}$ and the $2.21 \times 10^{-8}\ \text{A}$ at $-5\ \text{V}$, respectively).

The degradation in reverse characteristics is believed to be due to the time dependent plasma damage, where the surface damage increases as the exposure time of the LED surface to the plasma increases during the deposition of dielectric layers. The plasma damage may lead to the formation of lattice defects and/or dangling bonds at near-surface which results in the degradation in output power of LEDs as shown in **Figure 2(b)** [17,18].

The output power of the LED with $20\ \text{nm}$ -thick Al_2O_3 layer is considerably decreased compared to other LEDs with thinner Al_2O_3 layer. For this reason, the $5\ \text{nm}$ -thick Al_2O_3 layer was chosen to minimize the plasma damage. Additionally, the $5\ \text{nm}$ -thick Al_2O_3 layer plays a role of not only very effective passivation layer of the LED sur-



(a)



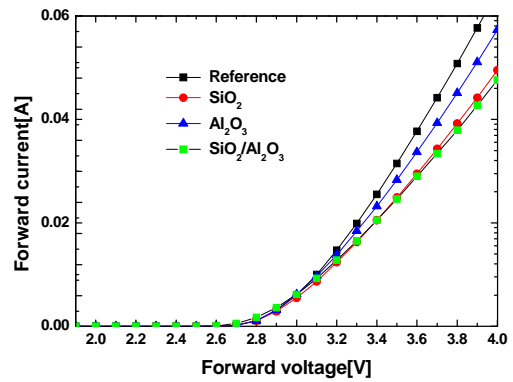
(b)

Figure 2. The the leakage current characteristics (a) and the output power characteristics (b) of the SiO_2 (50 nm)/ Al_2O_3 (5 nm), SiO_2 (50 nm)/ Al_2O_3 (7.5 nm), SiO_2 (50 nm)/ Al_2O_3 (10 nm), and SiO_2 (50 nm)/ Al_2O_3 (20 nm)-passivated LEDs, respectively.

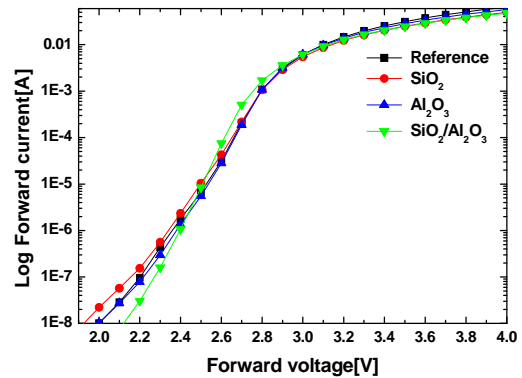
face but also partially anti-reflective layer in combination with 50 nm-thick SiO_2 layer even though the thickness is thinner than the calculated value for the anti-reflective layer. As a result, the total thickness for the double dielectric stack layer was optimized as 55 nm to achieve an efficient operation of the LED even though the thickness is not optimized for the maximum anti-reflectivity.

4. Results and Discussion

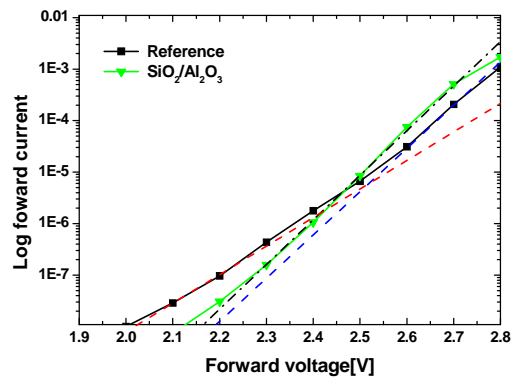
The linear and semi-log I-V characteristics of all fabricated LEDs are shown in Figures 3(a) and (b). The forward voltages measured at 20 mA were approximately 3.31, 3.33, 3.39 and 3.39 V for the non-passivated, the Al_2O_3 -passivated, the SiO_2 -passivated, and the $\text{SiO}_2/\text{Al}_2\text{O}_3$ -passivated LED, respectively. The forward voltages of the Al_2O_3 , the SiO_2 and the $\text{SiO}_2/\text{Al}_2\text{O}_3$ -passivated LEDs are slightly higher than that of the non-passivated LED. It is a little difficult to observe the difference in slopes between LEDs. To clearly see the difference, we compared the I-V curves for only two LEDs in (c) of the figure with the non-passivated LED and the $\text{SiO}_2/\text{Al}_2\text{O}_3$ double



(a)



(b)



(c)

Figure 3. The linear and semi-log I-V characteristics for all investigated LEDs at forward bias (a) and (b). To clearly see the difference, we compared the I-V curves for only two LEDs in (b) of the figure with non-passivated LED and the $\text{SiO}_2/\text{Al}_2\text{O}_3$ double dielectric passivated LED.

dielectric passivated LED. It is apparent that the non-passivated LED exhibits two characteristic lines, with a small slope at relatively low bias (<2.5 V) caused by which is equivalent to the surface shunt resistance and parasitic diode showing the prematured turn-on [19] as described later. On the other hand, the $\text{SiO}_2/\text{Al}_2\text{O}_3$ double dielectric passivated LED shows almost one dominant characteristic line with large slope, but the line with small slope disappears except at very low bias below ~ 2.2 V.

This explains that the I-V characteristic of the non-passivated LED is greatly affected by the existence of the shunt components at surface showing a hump in the curve, while that of the SiO₂/Al₂O₃ double dielectric passivated LED is less affected by these shunt components due to the effective surface passivation of the SiO₂/Al₂O₃ double dielectric layer. Therefore, the SiO₂/Al₂O₃ double dielectric passivated LED exhibits much more improved output power performance due to the decreased non-radiative recombination at surface. However, it is noticed that the SiO₂ passivated LED exhibits even worse I-V characteristic than that of the non-passivated one with even further prematured turn-on as shown in the figure. This is probably because the GaN surface becomes easily damaged when the surface is exposed to the plasma during the long deposition time, while the damage becomes minimized for the SiO₂/Al₂O₃ double dielectric passivation because the first thin Al₂O₃ layer deposited prior to the SiO₂ deposition prevents the GaN surface from being damaged. The GaN surface can be passivated with the deposition of the SiO₂ layer, which can be resulted in decrease of the effect of the shunt diode at surface. However, the plasma damage introduced during the deposition of the SiO₂ layer causes another surface leakage which is responsible for the worse I-V characteristic for the SiO₂ passivated LED. The passivation effect of the 5 nm-thick Al₂O₃ single dielectric layer is not remarkable compared to that of the double dielectric-passivation as shown in the **Figure 3(b)**. This is believed to be due to the insufficient surface passivation caused by nonuniform surface covering of the dielectric layer when the dielectric layer is very thin.

At a higher current level, however, the dielectric passivated LEDs exhibit larger series resistances than the non-passivated LED does as shown in the **Figure 4**.

The reason for the increased resistance with dielectric passivation can be understood by adopting an equivalent circuit model, as shown in **Figure 5(a)**, for the LED investigated in this work. The model consists of the main ideal bulk p-n diode (D₁), the contact resistance (R_C), the bulk series resistance (R_{SB}) mainly due to highly resistive p-type layer, the shunt resistance (R_{SS}), and the parasitic shunt diode (D₂) [19]. The shunt diode (D₂) and the shunt resistance (R_{SS}) are due to the surface leakage related to the surface states. The I-V characteristics of non-passivated LED can be inferred, considering all intrinsic and parasitic components. The I-V characteristics for D₁ (dotted-black line) can be degraded due to R_{SB} and R_C (dotted-blue line) as shown in **Figure 5(b)**. The curve for D₂ with R_{SS} is also shown as the dotted-green line in the figure. Therefore, the observable I-V characteristics for the non-passivated LED must be sum of the characteristics of the two diodes, shown as the dotted-red line in the figure.

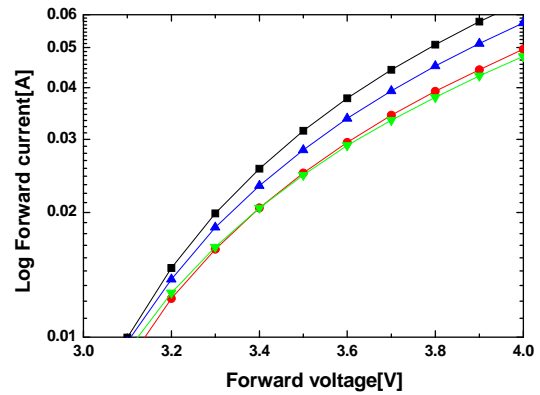
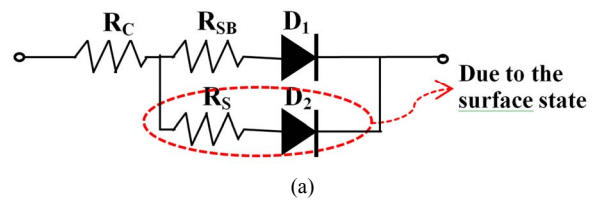
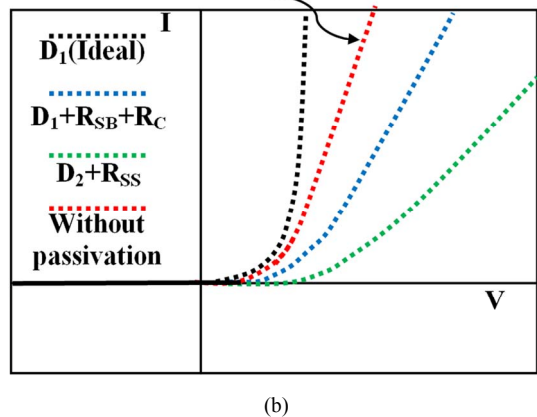


Figure 4. The semi-log I-V characteristics for all investigated LEDs at high forward bias.



The I-V characteristic of before passivation



The I-V characteristic of after passivation

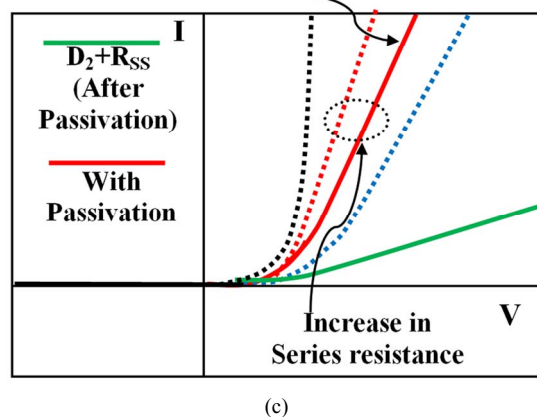


Figure 5. The Equivalent circuit model of the LED investigated in this work (a); the I-V characteristics of LEDs without (b); and with (c) passivation.

The I-V characteristics for D_1 with R_C and R_{SB} do not change even after passivation. However, the portion of D_2 with R_{SS} in the I-V characteristics becomes much reduced because the passivation layer greatly decreases the surface state density. This means that the effect of D_2 and R_{SS} on the total diode characteristics becomes less which can be visualized as green line in **Figure 5(c)**. Therefore, the I-V characteristics for the passivated LED, obtained from the sum of the characteristics of the two diodes (the broken blue line + the green line), can be drawn as red line in the figure, where the slope of the I-V curve is smaller than that of the I-V curve before the passivation, indicating that the series resistance of the passivated LED is larger than that of the non-passivated LED. The premature turn-on observed for the passivated LED is probably due to the surface leakage, which cannot be fully eliminated by the passivation, and/or additional shunt resistance, caused by plasma damage.

Figure 6 shows the reverse leakage current characteristics for the fabricated LEDs. As shown in the figure, the leakage current of the Al_2O_3 -passivated LED was -3.46×10^{-11} A at the -5 V, at least two and three orders lower in magnitude compared to that of the SiO_2 -passivated LED (-7.14×10^{-9} A) and the non-passivated LED (-1.9×10^{-8} A), respectively.

This indicates that the Al_2O_3 layer is very effective in passivating the exposed GaN surface after dry etch and hence decreases the trap density near the surface, which minimizes the leakage current through the surface of the LED. The trap density at the GaN surface was obtained by estimating the flatband voltage shift of the metal-insulator-semiconductor (MIS) capacitors, which depends on the polarity and the density of charges in the oxide and at the interface [20]. The measured C-V data were compared to the theoretical values using the Equation (3) below and the flatband voltage shift can be calculated.

$$V_{\text{FB}} = \Phi_{\text{M}} - \chi_{\text{S}} - \left[\frac{E_{\text{g}}}{2} - \frac{kT}{q} \ln \frac{N}{n_i} \right] - \frac{Q_{\text{F}}}{C_{\text{OX}}} - \frac{Q_{\text{IT}}}{C_{\text{OX}}} \quad (3)$$

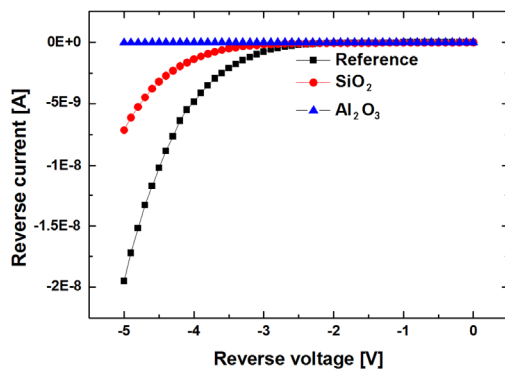


Figure 6. The LED with Al_2O_3 layer exhibits at least two and three orders lower in leakage current compared to that with SiO_2 layer and without dielectric layer, respectively.

where Φ_{M} is the metal work function, χ_{S} is the electron affinity of the semiconductor, E_{g} is the band gap energy, k is the Boltzmann constant, T is the temperature, q is the elementary charge, N is the doping density, n_i is the intrinsic carrier concentration, Q_{F} is the density of fixed charges, Q_{IT} is the density of interface trap charges, and C_{OX} is the oxide capacitance. The first three terms represent the ideal flatband voltage and the latter two causes the flatband voltage shift which depends on the polarity and the density of charges in the oxide and at the interface. The estimated interface trap density obtained from the Q_{IT} are shown in **Table 1**. The decreased trap density with Al_2O_3 passivation at the GaN surface leads to decrease in nonradiative surface recombination, which in turn increases the radiative efficiency and hence the output power from the LED.

Figure 7 shows the output powers versus currents for all LEDs studied in this work, which demonstrates the output powers of dielectric-passivated LEDs are higher than that of the non-passivated LED. The output power is 25.8, 26.5, 27.9, and 32.3 for the non-passivated, the SiO_2 -passivated, the Al_2O_3 -passivated, and the $\text{Al}_2\text{O}_3/\text{SiO}_2$ -passivated LED at $I_{\text{F}} = 100$ mA, respectively.

The reason for the higher output power for the dielectric passivated LED is because an additional transparent layer with refractive index n on NiAu/GaN as well as on the etched LED surface results in a larger critical angle for the emitted light. It is also noticed that the output power of the Al_2O_3 -passivated LED is slightly higher than

Table 1. Characteristics of interface charge density in GaN MIS structures.

material	value
Al_2O_3	$2.6 \times 10^{11} \text{ eV}^{-1} \cdot \text{cm}^{-2}$
SiO_2	$6.2 \times 10^{12} \text{ eV}^{-1} \cdot \text{cm}^{-2}$

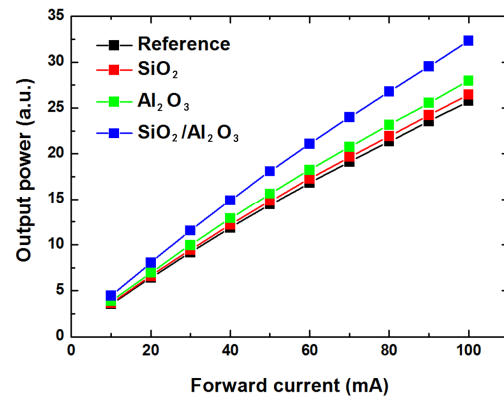


Figure 7. The output power characteristics of the non-passivated, the SiO_2 -passivated, the Al_2O_3 -passivated, and the $\text{Al}_2\text{O}_3/\text{SiO}_2$ -passivated LED. The output power of the $\text{Al}_2\text{O}_3/\text{SiO}_2$ -passivated LED exhibits about 25% higher than that of the non-passivated LED.

that of the SiO₂-passivated LED, which is unexpected and must be discussed, and the double dielectric Al₂O₃/SiO₂-passivated LED exhibits further enhanced output power. The output power of the SiO₂-passivated LED must be higher than that of the Al₂O₃-passivated LED, because the lower index of the SiO₂ layer deposited on the LED plays a role of increasing the light extraction efficiency due to larger critical angle factor as shown in **Table 2**, which is contrary to the result observed in **Figure 7**. According to the Snell's law, the critical angle (θ_{crit}) of total internal reflection is given by

$$\theta_{\text{crit}} = \sin^{-1}\left(\frac{n_2}{n_1}\right) \quad (4)$$

where n_1 and n_2 are the refractive indices of the semiconductor and air, respectively.

The reason why the Al₂O₃-passivated LED exhibits higher output power can be explained as follow; the Al₂O₃ layer covers whole surface of the LED, as shown in **Figure 1**, including the side-wall surface near the edge of the active quantum well exposed after plasma etching, except the n- and p-type contact. This Al₂O₃ layer effectively passivates the surface of the LED, which not only improves the electrical property of the LED by effectively reducing surface leakage as described before, but also reduces probability of nonradiative recombination through the surface trap and increases the radiative recombination efficiency in the active quantum well near side-wall edge. Furthermore, this passivation layer prevents the reabsorption of the emitted light near the surface regions. The surface passivation with Al₂O₃ layer, therefore, leads to increase of overall the external efficiency of the LED, even though the extraction efficiency of the Al₂O₃-passivated LED itself is lower than that of the SiO₂-passivated LED.

The output power of the Al₂O₃-passivated LED can be further increased by depositing additional 50 nm-thick SiO₂ layer on the Al₂O₃ layer to form the SiO₂/Al₂O₃ double dielectric stack layer. The output power of the LED with the double dielectric stack layer exhibits an output power, about 25.4% higher than that of the non-passivated LED and 15.6% higher than that of the Al₂O₃-passivated LED, respectively. This remarkable enhancement in output power of the LED with double dielectric passivation is because the first Al₂O₃ layer plays a role of effectively passivating the p-GaN surface and the second lower index SiO₂

layer plays a role of increasing the critical angle of the light emitted from the LED surface. In addition, the effect of the Fresnel reflection are also responsible for this enhancement in output power of the double dielectric passivated LED. Assuming normal incidence of light, the Fresnel power transmittance between GaN and air without any dielectric layer is given by

$$T = 1 - R = 1 - \left(\frac{n_{\text{GaN}} - n_{\text{air}}}{n_{\text{GaN}} + n_{\text{air}}}\right)^2 = \frac{4n_{\text{GaN}}n_{\text{air}}}{(n_{\text{GaN}} + n_{\text{air}})^2} \quad (5),$$

when thin dielectric layer, SiO₂ or Al₂O₃, is inserted between GaN and air, the transmittance can be expressed as below, neglecting multiple reflections between dielectric layers for simple calculation.

$$T = 1 - R = \frac{4n_{\text{GaN}}n_{\text{SiO}_2}}{(n_{\text{GaN}} + n_{\text{SiO}_2})^2} \times \frac{4n_{\text{SiO}_2}n_{\text{air}}}{(n_{\text{SiO}_2} + n_{\text{air}})^2}, \quad (6)$$

or

$$T = 1 - R = \frac{4n_{\text{GaN}}n_{\text{Al}_2\text{O}_3}}{(n_{\text{GaN}} + n_{\text{Al}_2\text{O}_3})^2} \times \frac{4n_{\text{Al}_2\text{O}_3}n_{\text{air}}}{(n_{\text{Al}_2\text{O}_3} + n_{\text{air}})^2}. \quad (7)$$

Similarly, when double dielectric stack layer, SiO₂/Al₂O₃, is inserted between GaN and air,

$$T = \frac{4n_{\text{GaN}}n_{\text{Al}_2\text{O}_3}}{(n_{\text{GaN}} + n_{\text{Al}_2\text{O}_3})^2} \times \frac{4n_{\text{Al}_2\text{O}_3}n_{\text{SiO}_2}}{(n_{\text{Al}_2\text{O}_3} + n_{\text{SiO}_2})^2} \times \frac{4n_{\text{SiO}_2}n_{\text{air}}}{(n_{\text{SiO}_2} + n_{\text{air}})^2} \quad (8)$$

where n_{GaN} , $n_{\text{Al}_2\text{O}_3}$, n_{SiO_2} , and n_{air} are the refractive indices of the GaN, Al₂O₃, SiO₂ and air, respectively. The above equations can be formalized as below:

$$T = 1 - R = \prod_{i=1}^3 \frac{4n_i n_{i+1}}{(n_i + n_{i+1})^2} \quad (9)$$

where $i = 1$ corresponds to the case without dielectric layer, $i = 2$ corresponds to the case with single dielectric layer (SiO₂ or Al₂O₃), and $i = 3$ corresponds to the case with double dielectric layer (SiO₂/Al₂O₃), respectively. From the above equation, the Fresnel power transmittances of the LED without a dielectric layer, with SiO₂, the Al₂O₃, and Al₂O₃/SiO₂ can be approximately calculated as 83.0%, 90.9%, 90.2%, and 93.5%, respectively. The calculated Fresnel power transmittance of the LED with double dielectric passivation, assuming normal incidence of the light, is approximately 10% higher than that that of non-passivated LED. This factor must be included in the improvement of the output power of the LED with double dielectric passivation, along with the contribution from the enhanced radiative recombination efficiency near side-wall edge as described before, which results in increase in the overall extraction efficiency from the LED.

Table 2. The critical angle calculated of dielectric deposited on GaN surface.

Passivation method	Critical angle
Al ₂ O ₃	34.4 degrees
SiO ₂	43.2 degrees
No dielectric	24.3 degrees

5. Conclusion

We have proposed a new concept of surface passivation for the GaN-based LED to improve the light extraction efficiency by using SiO₂/Al₂O₃ double dielectric stack layer and investigated its effects on the output power of the LED. The double dielectric stack layer not only effectively passivates the surface of the LED, but also enhances the overall extraction efficiency of the LED. The LED with the SiO₂/Al₂O₃ double dielectric stack layer exhibited about a 25.4% increase in the output power compared to the non-passivated LED.

6. Acknowledgements

This work was supported by Kyungpook National University Research Fund 2012, 2008 Brain Korea 21 (BK21), the National Research Foundation of Korea (NRF) grant funded by the Korea government (MEST) (No. 2012-0005671, 2012-0000627), R & D program of MKE/KETEP (2011101050017B, "Development of high efficiency GaN power device for an power grid inverter system"), and WCU (World Class University) program through the Korea Science and Engineering Foundation funded by the Ministry of Education, Science and Technology (R33-10055), and the IT R & D program of MKE/KEIT (10038766, Energy Efficient Power Semiconductor Technology for Next Generation Data Center).

REFERENCES

- [1] T. Fujii, Y. Gao, R. Sharma, E. L. Hu, S. P. Den Baars and S. Nakamura, "Increase in the Extraction Efficiency of GaN-Based Light-Emitting Diodes via Surface Roughening," *Applied Physics Letters*, Vol. 84, No. 6, 2004, pp. 855-857. [doi:10.1063/1.1645992](https://doi.org/10.1063/1.1645992)
- [2] C. M. Yang, D. S. Kim, S. G. Lee, J. H. Lee, Y. S. Lee and J. H. Lee, "Improvement in Electrical and Optical Performances of GaN-Based LED with SiO₂/Al₂O₃ Double Dielectric Stack Layer," *IEEE Electron Device Letters*, Vol. 33, No. 4, 2012, pp. 564-566. [doi:10.1109/LED.2012.2185675](https://doi.org/10.1109/LED.2012.2185675)
- [3] H.-W. Huang, C. C. Kao, J. T. Chu, S. C. Wang and C. C. Yu, "Improvement of InGaN-GaN Light-Emitting Diode Performance with a Nano-Roughened p-GaN Surface," *IEEE Photonics Technology Letters*, Vol. 17, No. 5, 2005, pp. 983-985. [doi:10.1109/LPT.2005.846741](https://doi.org/10.1109/LPT.2005.846741)
- [4] C. M. Tsai, J. K. Sheu, W. C. Lai, Y. P. Hsu, P. T. Wang, C. T. Kuo, C. W. Kuo, S. J. Chang and Y. K. Su, "Enhanced Output Power in GaN-Based LEDs with Naturally Textured Surface Grown by MOCVD," *IEEE Electron Device Letters*, Vol. 26, No. 7, 2005, pp. 464-466. [doi:10.1109/LED.2005.851243](https://doi.org/10.1109/LED.2005.851243)
- [5] M. Y. Hsieh, C. Y. Wang, L. Y. Chen, T. P. Lin, M. Y. Ke, Y. W. Cheng, Y. C. Yu, C. P. Chen, D. M. Yeh, C. F. Lu, C. F. Huang, C. C. Yang and J. J. Huang, "Improvement of External Extraction Efficiency in GaN-Based LEDs by SiO₂ Nanosphere Lithography," *IEEE Electron Device Letters*, Vol. 29, No. 7, 2008, pp. 658-660. [doi:10.1109/LED.2008.2000918](https://doi.org/10.1109/LED.2008.2000918)
- [6] J. H. Lee, J. T. Oh, S. B. Choi, Y. C. Kim, H. I. Cho and J. H. Lee, "Enhancement of InGaN-Based Vertical LED with Concavely Patterned Surface Using Patterned Sapphire Substrate," *IEEE Photonics Technology Letters*, Vol. 20, No. 5, 2008, pp. 345-347. [doi:10.1109/LPT.2007.915648](https://doi.org/10.1109/LPT.2007.915648)
- [7] J. H. Lee, J. T. Oh, Y. C. Kim and J. H. Lee, "Stress Reduction and Enhanced Extraction Efficiency of GaN-Based LED Grown on Cone-Shape-Patterned Sapphire," *IEEE Photonics Technology Letters*, Vol. 20, No. 18, 2008, pp. 1563-1565. [doi:10.1109/LPT.2008.928844](https://doi.org/10.1109/LPT.2008.928844)
- [8] C. F. Shen, S. J. Chang, W. S. Chen, T. K. Ko, C. T. Kuo and S. C. Shei, "Nitride-Based High-Power Flip-Chip LED with Double-Side Patterned Sapphire Substrate," *IEEE Photonics Technology Letters*, Vol. 19, No. 10, 2007, pp. 780-782. [doi:10.1109/LPT.2007.896574](https://doi.org/10.1109/LPT.2007.896574)
- [9] S. H. Huang, R. H. Horng, K. S. When, Y. F. Lin, K. W. Yen and D. S. Wu, "Improved Light Extraction of Nitride-Based Flip-Chip Light-Emitting Diodes via Sapphire Shaping and Texturing," *IEEE Photonics Technology Letters*, Vol. 18, No. 24, 2006, pp. 2623-2625. [doi:10.1109/LPT.2006.886823](https://doi.org/10.1109/LPT.2006.886823)
- [10] O. B. Shchekin, J. E. Epler, T. A. Trottier, T. Margalith, D. A. Steigerwald, M. O. Holcomb, P. S. Martin and M. R. Krames, "High Performance Thin-Film Flip-Chip InGaN-GaN Light-Emitting Diodes," *Applied Physics Letters*, Vol. 89, No. 7, 2006, Article ID: 071109. [doi:10.1063/1.2337007](https://doi.org/10.1063/1.2337007)
- [11] S. J. Wang, K. M. Usang, S. L. Chen, Y. C. Yang, S. C. Chang, T. M. Chen, B. W. Liou and C. H. Chen, "Use of Patterned Laser Lift-off Process and Electroplating Nickel Layer for the Fabrication of Vertical-Structured GaN-Based Light-Emitting Diodes," *Applied Physics Letters*, Vol. 87, 2005, Article ID: 011111. [doi:10.1063/1.1993757](https://doi.org/10.1063/1.1993757)
- [12] H. W. Huang, C. H. Lin, Z. K. Huang, K. Y. Lee, C. C. Yu and H. C. Kuo, "Improved Light Output Power of GaN-Based Light-Emitting Diodes Using Double Photonic Quasi-Crystal Patterns," *IEEE Electron Device Letters*, Vol. 30, No. 11, 2009, pp. 1152-1154. [doi:10.1109/LED.2009.2029985](https://doi.org/10.1109/LED.2009.2029985)
- [13] M. F. Schubert, F. W. Mont, S. Chhajed, D. J. Poxson, J. K. Kim and E. F. Schubert, "Design of Multilayer Anti-reflection Coatings Made from Co-Sputtered and Low-Refractive-Index Materials by Genetic Algorithm," *Optics Express*, Vol. 16, No. 8, 2008, pp. 5290-5298. [doi:10.1364/OE.16.005290](https://doi.org/10.1364/OE.16.005290)
- [14] J.-Q. Xi, M. F. Schubert, J. K. Kim, E. F. Schubert, M. Chen, S.-Y. Lin, W. Liu and J. A. Smart, "Optical Thin-Film Materials with Low Refractive Index for Broadband Elimination of Fresnel Reflection," *Nature Photonics*, Vol. 1, No. 3, 2007, pp. 176-179.
- [15] S.-J. So and C.-B. Park, "Improvement of Brightness with Al₂O₃ Passivation Layers on the Surface of InGaN/GaN-Based Light-Emitting Diode Chips," *Thin Solid Film*, Vol. 516, No. 8, 2008, pp. 2031-2034.

- [doi:10.1016/j.tsf.2007.07.143](https://doi.org/10.1016/j.tsf.2007.07.143)
- [16] C. Ostermaier, H.-C. Lee, S.-Y. Hyun, S.-I. Ahn, K.-W. Kim, H.-I. Cho, J.-B. Ha and J.-H. Lee, "Interface Characterization of ALD Deposited Al₂O₃ on GaN by CV Method," *Physica Status Solidi*, Vol. 5, No. 6, 2008, pp. 1992-1994.
- [17] Y. Li, X. Y. Yi, X. D. Wang, J. X. Guo, L. C. Wang, G. H. Wang, F. H. Yang, Y. P. Zeng and J. M. Li, "Plasma Induced Damage in GaN-Based Light Emitting Diodes," *SPIE Proceedings*, Vol. 6841, 2007, Article ID: 68410x. [doi:10.1117/12.759809](https://doi.org/10.1117/12.759809)
- [18] H. S. Yang, S. Y. Han, K. H. Baik and S. J. Pearton, "Effect of Inductively Coupled Plasma Damage on Performance of GaN-InGaN Multiquantum-Well Light-Emitting Diodes," *Applied Physics Letters*, Vol. 86, 2005, Article ID: 102104. [doi:10.1063/1.1882749](https://doi.org/10.1063/1.1882749)
- [19] E. F. Schubert, "Light-Emitting Diodes," 2nd Edition, Cambridge University Press, Cambridge, 2006. [doi:10.1017/CBO9780511790546](https://doi.org/10.1017/CBO9780511790546)
- [20] K. Matocha, R. J. Gutmann and T. P. Chow, "Effect of Annealing on GaN-Insulator Interfaces Characterized by Metal-Insulator-Semiconductor Capacitors," *IEEE Transactions on Electron Devices*, Vol. 50, No. 5, 2003, pp. 1200-1204. [doi:10.1109/TED.2003.813456](https://doi.org/10.1109/TED.2003.813456)